Experiments on Hypersonic Lifting Bodies

L. F. CRABTREE AND D. A. TREADGOLD
Royal Aircraft Establishment, Farnborough

SUMMARY

This paper reports on wind-tunnel studies of simple delta-like shapes which might form the basis of future hypersonic aircraft. The tests ranged from low-speed (150 ft/sec) through supersonic ($M = 2{\cdot}47$ and $4{\cdot}30$) to hypersonic speed ($M = 8{\cdot}6$), and in general attention was concentrated on wave-rider shapes, including flat-bottomed delta wings.

The low-speed tests covered longitudinal and lateral stability, and all the shapes tested showed satisfactory handling qualities for typical landing conditions.

The supersonic tests concentrated on off-design performance of inverted-V or caret wave-rider wings, and showed that a uniform under-surface flow can be achieved over a wide range of off-design incidence and Mach number.

Finally, the tests at hypersonic speeds show that maximum lift-to-drag ratios in cruise of over 4 (excluding base-drag) can be obtained, and some simple calculations show that this enables global ranges to be achieved with hydrogen ram-jet propulsion and cruise Mach numbers of the order of 8 to 10.

1. INTRODUCTION

Hypersonic aircraft show considerable promise of providing really long ranges (over 8000 miles say) in the future. As a first step in understanding the major aerodynamic problems involved in the design of such an aircraft a series of wind-tunnel tests have been carried out over the complete speed range on some simple idealised shapes, which may yet provide the basis of a practical design.

Some of the shapes tested take advantage of one or other of the methods that have been suggested over the past few years for designing the shapes of

lifting bodies to support known inviscid supersonic and hypersonic flow fields. Usually the shape is designed to support a shock system which is contained below it and between the leading edges. The term wave-rider has been coined to describe such designs, the simplest of which is the caret or inverted-V wing, suggested by Nonweiler, which contains a plane oblique shock wave. The various possibilities have been described by Kuchemann[1], but it may be worth repeating here some of the advantages of this approach.

Apart from viscosity effects, the pressure distribution over a large part of the surface is specified exactly at the design condition. This avoids the difficulties and inaccuracies associated with the use of approximate theories to calculate pressure over bodies of arbitrary shape; it also allows the choice of suitable distributions of pressure and loading, with a view to obtaining low pressure drag, for example. There remains an off-design problem when the pressures have to be determined at Mach numbers and attitudes which differ from the design condition, but it is some help that these flows may be regarded as departures from a known design flow field.

Again, since the caret wing, for instance, has been shown[2] to provide near-optimum aerodynamic efficiency in terms of maximum lift-to-drag ratio, it may be hoped that a practical design will differ only in modifications to adapt the lengthwise volume distribution to practical requirements, for instance. Thus the flow field would again be only a departure from a known design case. Finally, it is a considerable advantage to be able to present a uniform flow to the engine face, as is automatically provided by the caret wing.

The low-speed tests described in section 2 were done by Keating and Mayne[3]. in the 13 ft × 9 ft wind-tunnel at R.A.E. Bedford. These concentrated on delta-like shapes with a flat bottom and triangular cross-section, but one model was of a cone-flow wave-rider designed by the method of Jones[4].

The supersonic tests were carried out by Treadgold[5] in a 10 in × 9 in tunnel at R.A.E. Farnborough. As described in section 3, these tests were intended to investigate the off-design characteristics of caret wave-riders.

The hypersonic tests (section 4) were done by Crane[6] in the 7 in × 7 in tunnel at R.A.E. Farnborough, and illustrate the comparison between a caret wing and flat-bottomed delta wings with the same volume parameter, $\tau = V/S^{3/2}$, of 0·06 where V is volume and S the plan area, and the same aspect ratio (in fact, A.R. = 1).

Finally, section 5 gives the results of a recent study[7] of the range performance of hypersonic aircraft allowing for the climb and glide phases. These simple calculations are sufficient to show the potential of such aircraft for achieving global ranges using liquid hydrogen fuel, a Mach number around 8 and a lift-to-drag ratio of 4 or more.

Symbols

C_f skin friction coefficient
C_p base pressure coefficient
l model length
M_d design Mach number for caret wings
M_∞ free stream Mach number
S plan area
s semi-span
V volume
α incidence angle
β sideslip angle
δ flow deflection angle
δ_n flow deflection angle in a plane normal to the leading edge
ζ shock wave angle
ζ_n shock wave angle in a plane normal to the leading edge
τ volume parameter $\tau = V/S^{3/2}$

2. Low-Speed Characteristics of Hypersonic Shapes

A series of models was designed to provide some guidance on the limitations imposed by considerations of low-speed performance on the choice of cone-flow wave-rider planform shapes from the inherently large range possible. Previous low-speed studies have given guidance on delta, gothic and ogee planforms, but it is possible to obtain, from the design method for supersonic cruise[4], planforms outside this experience, particularly in the degree of 'bluntness' at the apex.

Present thoughts are in terms of delta-like shapes for all the wave-rider types with values of slenderness ratio, s/l = semi-span/length, between about 0·2 and 0·3. This has been shown to be the range of interest from cruise considerations[1], so we are dealing with non-slender shapes (at cruise) where s/l is not too small for satisfactory low-speed qualities, and basically with sharp edges. Hence, at low speeds, vortex flow exists on the upper surface with the shapes involving non-zero edge angle, droop and possibly some change of sweep angle along the leading-edge. We know that in principle orderly and controllable flow can be obtained but the actual details (C_L, C_D, C_m, vortex breakdown etc.) need to be studied. The present investigation was aimed primarily at achieving a satisfactory development of the separated flow field over the upper surface of the wing up to suitably high angles of attack. Thus the model planforms were designed to investigate the effect of

planform nose shape on wings of constant slenderness ratio ($s/l=0{\cdot}4663$, corresponding to a 65° delta). The models are simplified forms of wave-rider wings, having plane under surfaces and a triangular spanwise thickness distribution. A single, fully representative, model of a wave-rider with the camber and thickness distribution obtained from conical shock and expansion theory[4] completed the series. Some of the models are rather extreme ($s/l=0{\cdot}47$ for instance) just to see how far one could go. Incidentally, the flat-bottom wings are also wave-riders in a sense, for they have an attached shock over quite a range of incidence and Mach number.

The tests involved six-component force measurements as well as oil-flow and smoke visualisation tests to try to establish the nature of the separated flow field. Attempts were also made to study the velocity distribution through the vortex cores on some of the wings, in particular to establish the nature of an unusual 'vortex-breakdown', demonstrated by smoke on the more blunt-nose planforms.

Figures 1 and 2 show the planform shapes and the thickness distribution respectively of the wing. Models *A* and *B* were intended as reference models to relate the results of the present tests with flat plate results, and are slender deltas with leading-edge sweeps of 65° and 70°. The remaining models have the same slenderness ratio as the 65° delta. Models *C*, *D* and *E* have zero sweep at the nose, increasing to 67·5°, 70° and 72·5° respectively at the trailing-edge. Models *H*, *G* and *F* have a constant angle of sweepback at the trailing-edge of 70° with sweeps at the nose of 20°, 40° and 60° respectively.

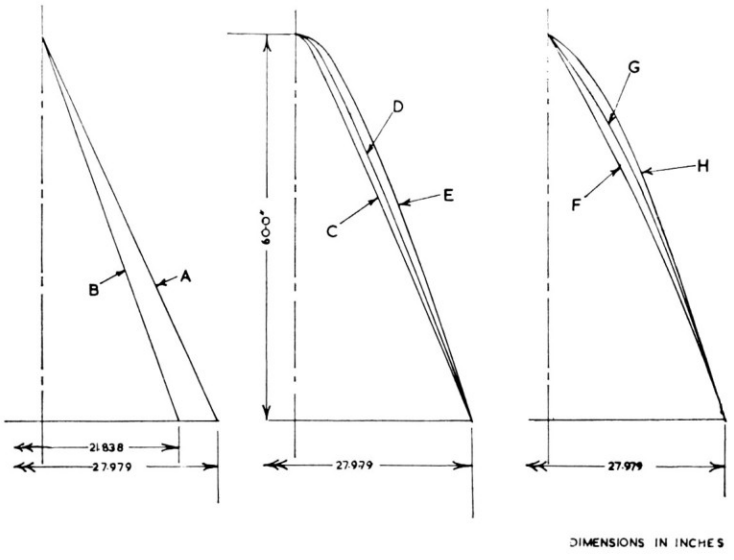

FIG. 1 — Wing planforms for low-speed tests

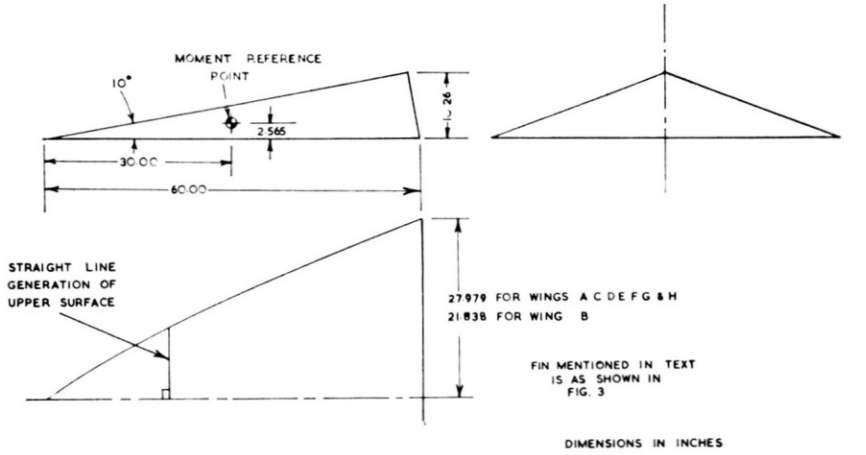

FIG. 2 — Low-speed model geometry

Fuller details are given in a forthcoming report[3]. Fig. 3 shows the fully representative model of a cone-flow wave-rider wing.

An interesting aspect that came to light during the tests was the nature, and early occurrence, of vortex breakdown on wings with 'blunt' planforms. Vortex breakdown usually presents itself as a loss of non-linear lift at the trailing edge shown by a loss of gross lift and a reduction in longitudinal static stability (pitch-up), accompanied by unsteadiness of the flow. The lift and pitching moment curves for the whole series of models are shown in Figs. 4 and 5, and the curves for the delta wing *A* provide a typical illustration of the above description of vortex breakdown. In this case, a pitch-up and reduction in lift-curve slope occur at lift coefficients above about 0·6. However, the results for wings *C*, *D* and *E* indicate that the effect of progressive blunting of the apex reduces the severity of these effects, in spite of an apparent increase in the amount of non-linear lift generated.

Smoke injected into the vortex near the apex gave some indication of the character of the wing vortices and some of the results are shown in Fig. 6. The reduction in severity of the vortex 'burst' with increase of planform bluntness at the apex is clearly seen. For the bluntest shape tested, wing *E*, there is apparently none of the visual characteristic core expansion associated with breakdown, and a comparatively gradual diffusion of the 'smoke tube' occurs. Apart from a small region near the apex in this case the entire vortex field appeared to be in this 'burst' state over the whole incidence range and the possible co-existence of a vigorous external 'vortex' flow (associated with the development of non-linear lift) with a diffuse low-energy core needs more investigation. Attempts have been made to determine something of the vortex structure using a traversing probe and the results analysed so far indicate that this type of structure does exist.

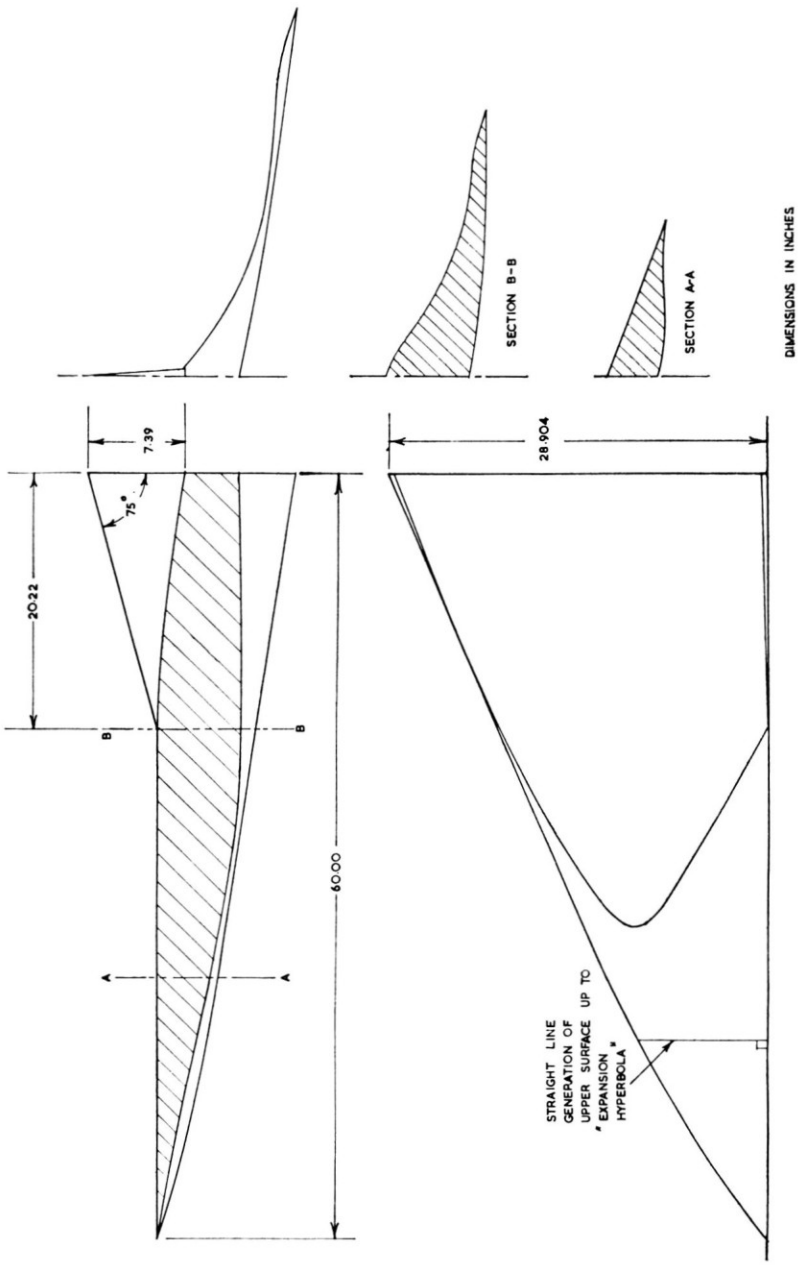

FIG. 3 — Cone-flow wave-rider for low-speed tests

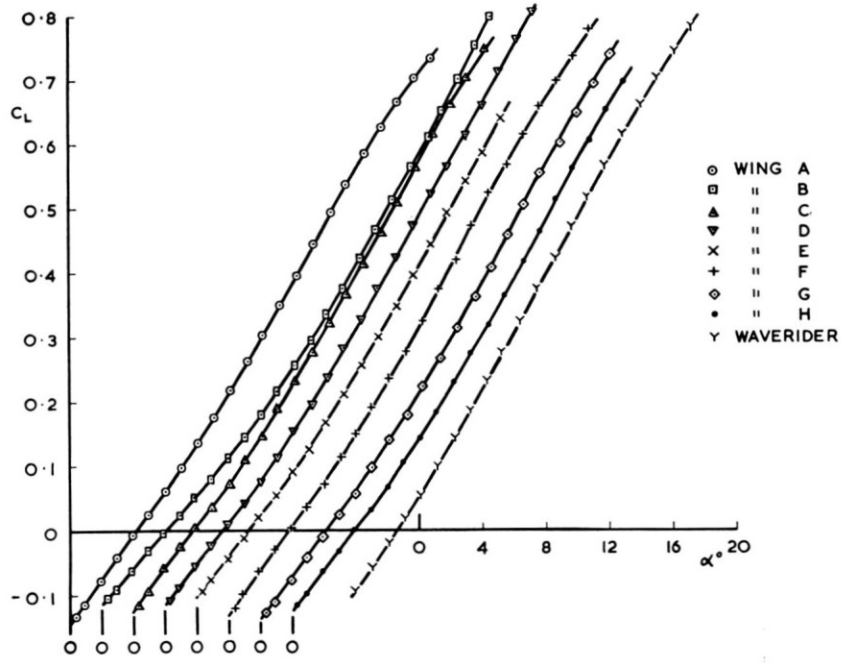

FIG. 4 — Lift curves for low-speed models

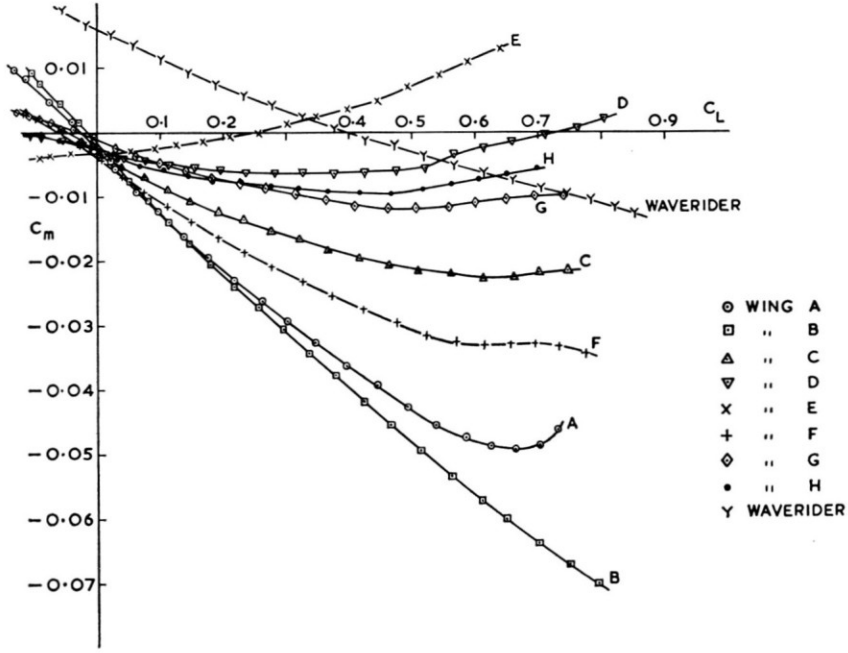

FIG. 5 — Pitching moment curves for low-speed models

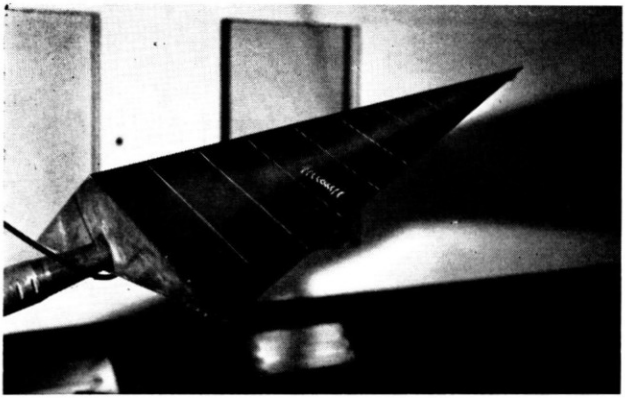

Model A
$\alpha = 22°$
$\beta = 0$

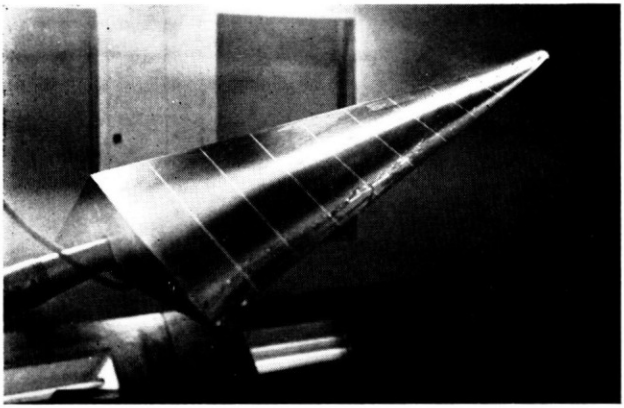

Model C
$\alpha = 22°$
$\beta = 5°$

Model E
$\alpha = 22°$
$\beta = 10°$

FIG. 6 — Visualisation of wing vortices by smoke flow

One aspect on which doubt was expressed early in the programme was the stable or rather symmetrical development of the separated flow field at low angles of attack in sideslip. Oil flow tests, illustrated in Fig. 7, showed that the vortices did develop asymmetrically, but all the indications are that the effect on the forces on the wing is negligible, due to the weakness of the vortices at such low angles of attack.

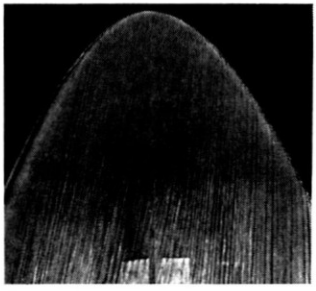

$\alpha = 5°, \beta = 8°$

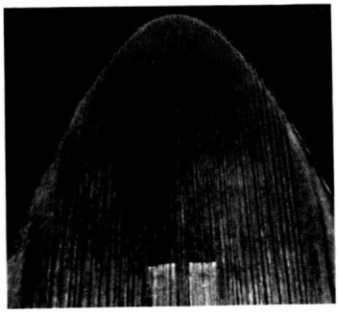

$\alpha = 5°, \beta = 0$

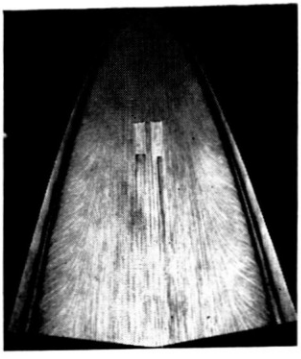

$\alpha = 16°, \beta = 0$

FIG. 7 — Surface oil flow pictures showing effect of sideslip on wing vortices (model *E*)

Finally, measurements were made of yawing and rolling moments, with and without fin. These are plotted as coefficients in Fig. 8, for a typical case (model *E*). The corresponding lateral derivatives l_v and n_v as shown in Fig. 9 suggest no great handling difficulties for typical landing conditions, but at small incidences where $l_v/n_v > 0$ a degree of spiral instability will have to be tolerated.

o

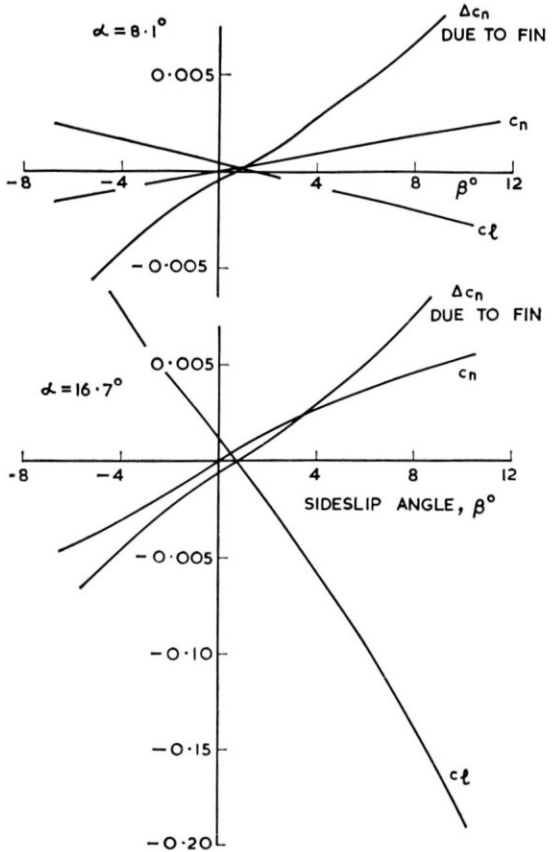

FIG. 8 — Low-speed lateral stability characteristics of wing *E*

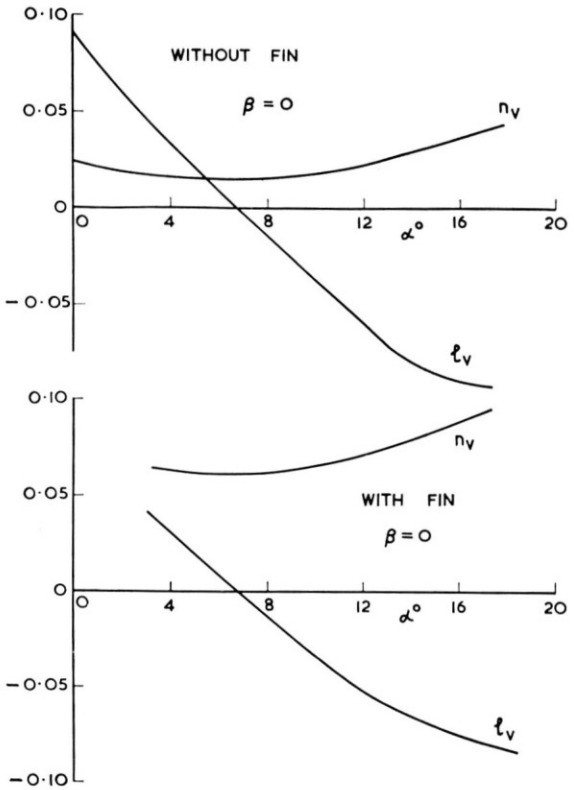

FIG. 9 — Low-speed lateral stability derivatives of wing *E*

3. Supersonic Tests of Caret Wave-Riders

The models tested in the supersonic tunnel are shown in Fig. 10, the principal aim being to investigate the off-design characteristics of simple caret or inverted-V wings. All the models have a streamwise upper surface in the design condition, and their geometry is defined by the parameters δ the flow deflection angle, M_d the design Mach number, and A the aspect

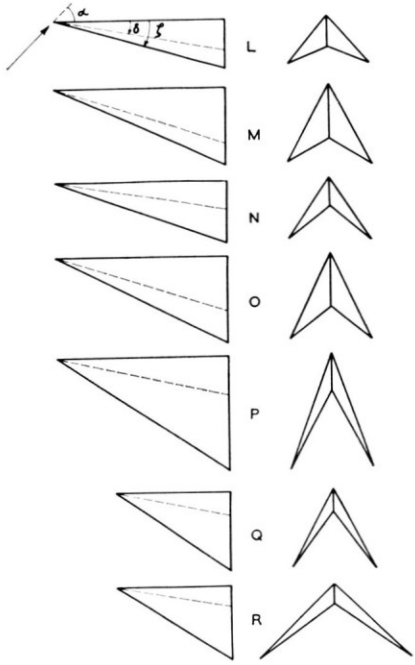

Fig. 10 — Supersonic tunnel models

ratio. These values are given in Table 1, together with the corresponding values of the shock wave angle ζ, and the volume parameter $\tau = \text{volume}/(\text{plan area})^{3/2}$. Some of the shapes have rather large values of τ. Whereas wing N corresponds roughly to a typical hydrogen fuelled aircraft (*see* section 5), wing O for instance is much too thick.

The design conditions were checked by measurements of the pressure distribution. On the lower surface, these confirmed the uniform pressure expected, the level being slightly higher than the design value as calculated from the inviscid oblique shock wave equations. This slight difference is

TABLE 1

DESIGN PARAMETERS FOR CARET WING TUNNEL MODELS

Model	*Design Mach number* M_d	*Flow Deflection Angle* δ°	*Shock Wave Angle* ζ°	*Design* C_L	*Aspect Ratio* A	*Volume Coefficient* τ
L	6·85	10·15	16·68	0·10	1·0	0·120
M	6·85	17·73	25·02	0·25	1·0	0·226
N	4·30	8·41	19·80	0·10	1·0	0·099
O	4·30	16·17	27·3	0·25	1·0	0·193
P	2·47	12·13	34·28	0·25	1·0	0·143
Q	2·47	12·13	34·28	0·25	1·5	0·117
R	2·47	12·13	34·28	0·25	2·73	0·087
Z†	6·85	10·1	16·6	0·10	1·0	0·060

† The model used in the hypersonic tests was designed for a particular value of τ, therefore it did not have a streamwise upper surface.

partially accounted for by crude strip theory estimates of the displacement effect of the boundary layer. On the upper surface, this simple strip theory again underestimated the pressures induced by the boundary-layer displacement effect.

The design point is, of course, not necessarily the attitude for maximum L/D, as can be seen from Fig. 11(*a*) and (*b*) which show typical curves of

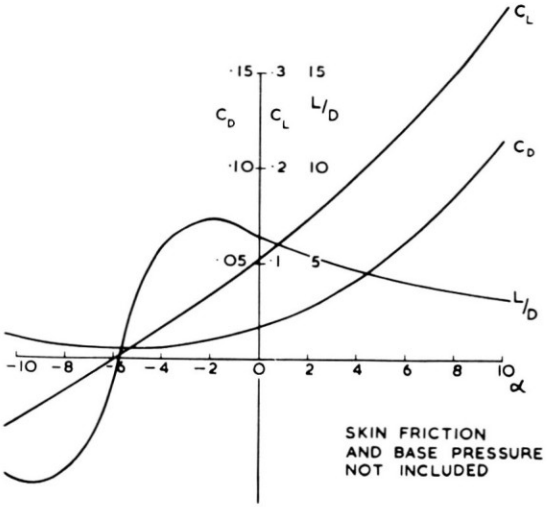

FIG. 11(*a*) — Typical C_L, C_D and L/D curves for model *N*

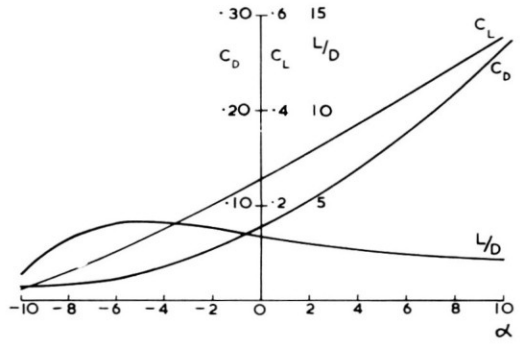

FIG. 11(*b*) — Typical C_L, C_D and L/D curves for model *O*, skin friction and base pressure not included

C_L, C_D and L/D. This can also be shown quite readily by assuming the Busemann expansion for pressures on the upper and lower surfaces. We find that

$$\alpha_{(L/D_{max})} = -\tfrac{1}{2}\delta + \tfrac{1}{2}\left(\frac{2C_1\delta^2 + C_2\delta^3 + 4C_{D_f}}{2C_1 + 3C_2\delta}\right)^{1/2}$$

where C_1 and C_2 are the familiar Busemann coefficients,

$$C_1 = 2(M_\infty^2 - 1)^{-1/2}$$

and

$$C_2 = \frac{(\gamma+1)M_\infty^4 - 4(M_\infty^2 - 1)}{2(M_\infty^2 - 1)^2}$$

Thus for small deflection angles and negligible friction drag, the optimum incidence tends to $-\delta/2$, but skin friction and base drag (neither of which have been taken into account in Fig. 11) would both tend to bring the optimum incidence nearer to the design value.

Now the design condition corresponds to the trivial case of uniform flow; so it is of no consequence whether the flow downstream of the leading-edges is conically supersonic or subsonic, but this is of great importance in off-design conditions. In the former case the equation of inviscid flow over the under-surface has a hyperbolic region which may be bounded by further shock waves, while the flows over the two leading edges are mutually independent. In the conically subsonic case the equation is in general elliptic; no further discontinuities in the pressure field need to exist, and the two leading edges are no longer independent.

An illustration of the further shock which can form in the conically supersonic case is given in Fig. 12. This is a caret wing at its design incidence but

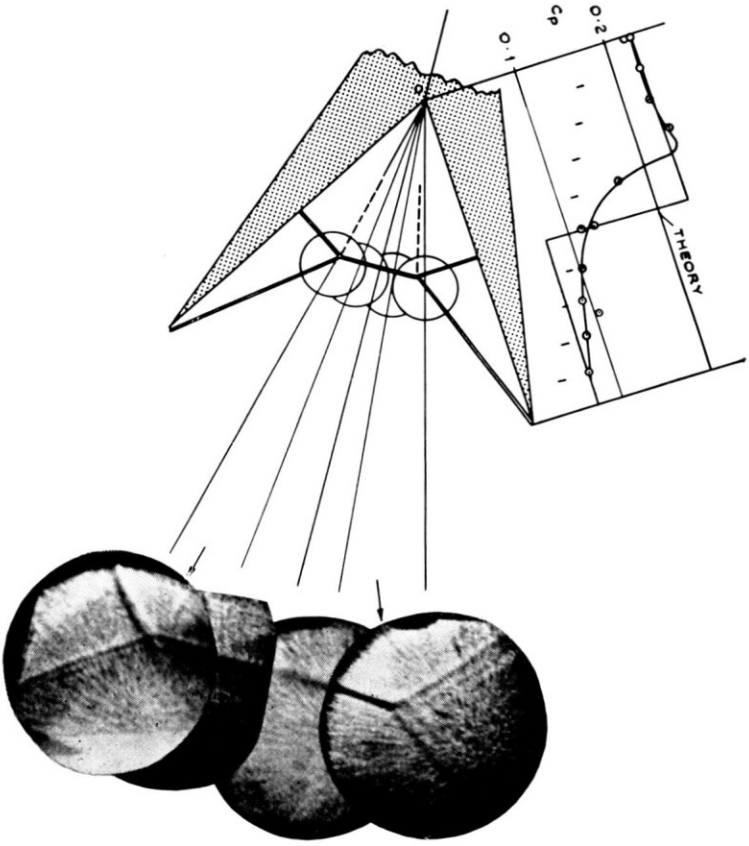

FIG. 12 — Conical shadowgraph of wing *P* at a Mach number of 4·3 and zero incidence

above its design Mach number. The figure shows a conical shadowgraph which clearly indicates the existence of a shock wave corresponding to the rapid rise in surface pressure at about mid-semispan. The photographs also show some evidence of the vortex sheet which emanates from the intersection of the three shock waves. This further shock wave is similar to the one which has been observed inboard of the hyperbolic region on the expansion surface of a delta wing[8].

A crude theoretical model may be constructed by assuming the existence of a single oblique shock which turns the airstream parallel to the plane of symmetry, since after passing through the leading-edge shock the flow has a fairly large component towards the ridge line. This model appears to give a reasonably good estimate of the pressure at the centre-line, although the discontinuous pressure change is smoothed out in practice. Further examples

are given in Fig. 13, where some spot points from free-flight experiments by Picken and Greenwood[9] have also been marked. Under these conditions of operation, well above the design Mach number, the feature of a uniform pressure field is clearly no longer retained. However, it must be appreciated that the examples given correspond to gross off-design conditions.

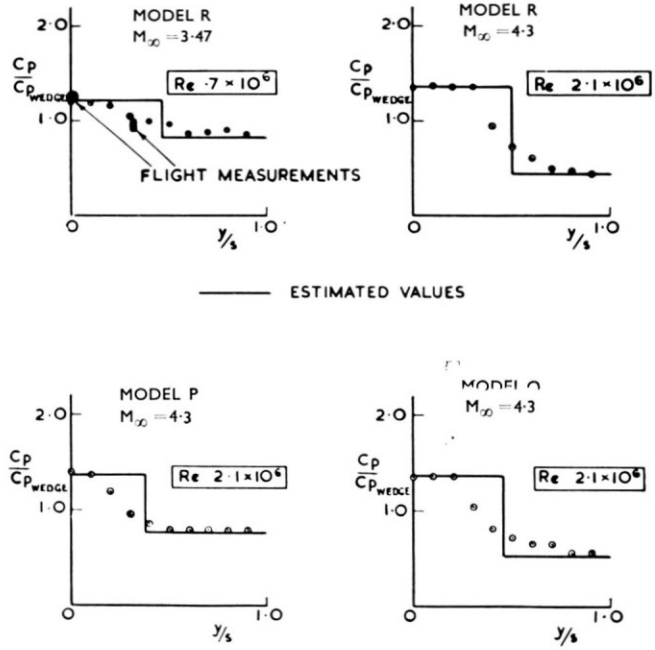

FIG. 13 — Pressure distributions at the design incidence but at Mach numbers above the design value

Let us now consider the case of a wing at its design Mach number but not at its design incidence (defined by $\alpha = 0$). The example in Fig. 14 is of wing *N* designed for a Mach number of 4·3 with the upper surface streamwise and a lower surface ridge angle of $\delta = 8{\cdot}4°$. It will be seen that the pressure over the lower surface remains practically constant across the span for a range of pressure coefficients from zero up to about 3 times the design value. Calculations have been made of the pressures near the leading edge using the oblique shock-wave relationships and assuming the leading edges to be independent. The results are shown in Fig. 15. It will be seen that at negative incidence the deflection of the flow at the leading edge is only slightly away from the plane of symmetry whereas at positive incidence the flow is directed towards the plane of symmetry. This again suggests the use of the flow model previously described with the assumption that the flow is discontinuously

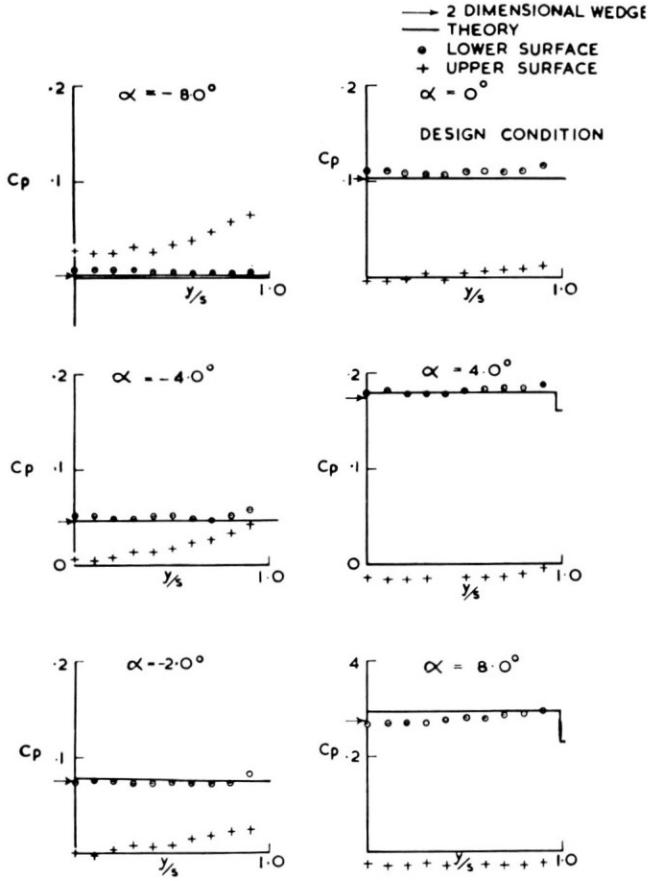

FIG. 14 — Pressure distributions at off-design incidence but at $M_d = 4{\cdot}3$ for wing N
(Re = 2·1 × 10-)

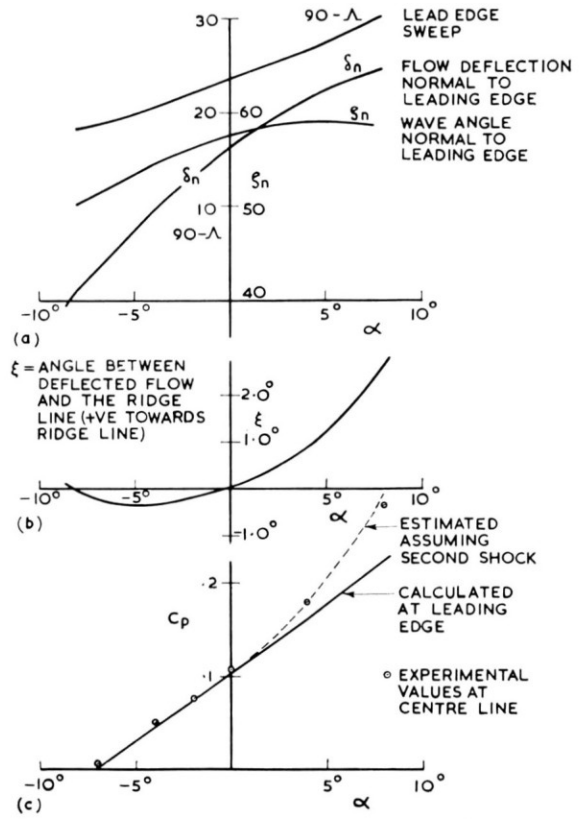

FIG. 15 — Calculated values of flow conditions near the leading-edge of wing N at off-design incidence but at $M_d = 4{\cdot}3$

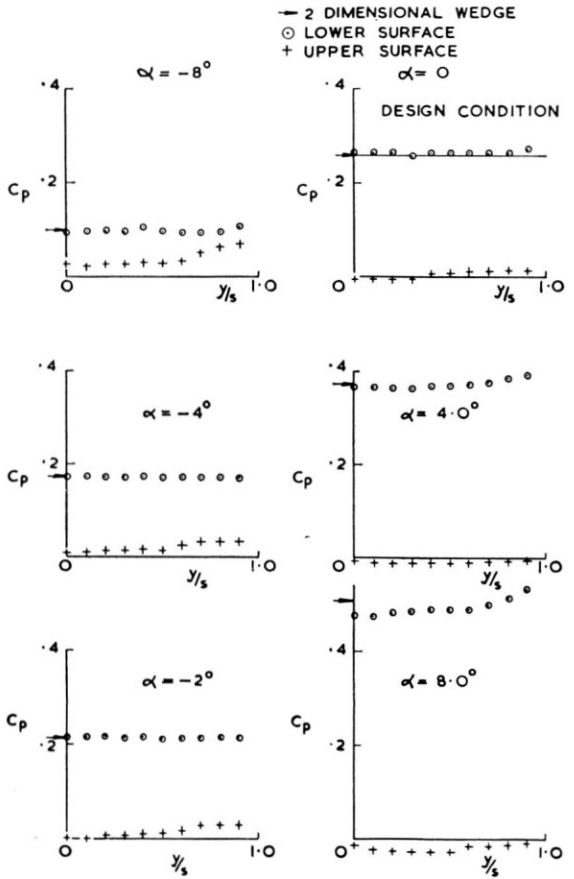

FIG. 16 — Pressure distribution on wing O at off-design incidence but at $M_d = 4{\cdot}3$

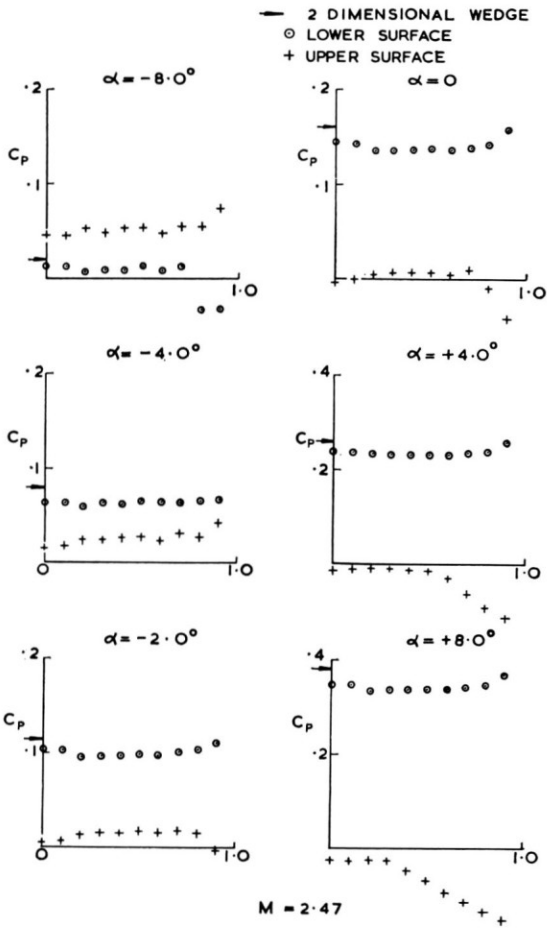

FIG. 17 — Pressure distributions on wing N at off-design incidence and at a Mach number below the design value

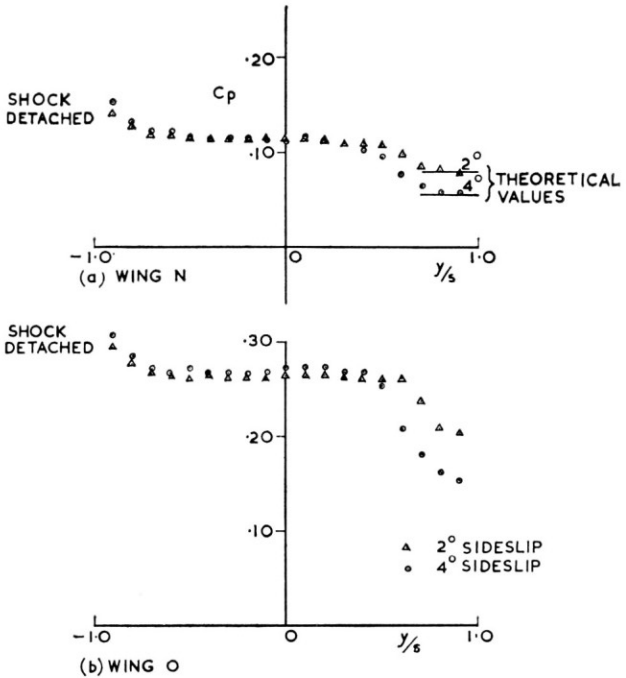

FIG. 18 — Effects of sideslip at the design incidence and Mach number

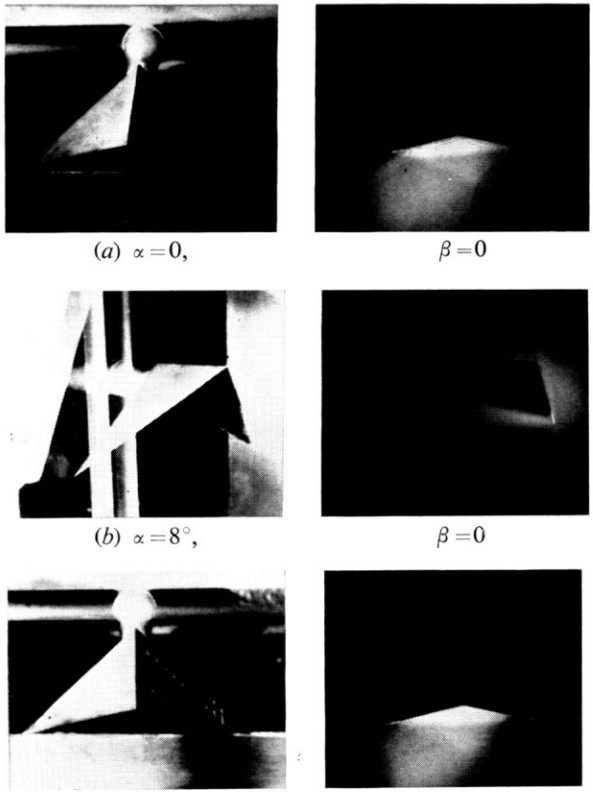

FIG. 19 — Vapour screen photographs, model *R* at $M = 2{\cdot}47$

turned parallel to the plane of symmetry. Fig. 15 shows that this gives a good prediction of the pressure on the centre-line.

Figure 16 shows the case of a design where the flow after the shock is conically subsonic. Here, it is not possible to use the above method of estimation in the off-design case since the leading-edges are no longer independent. However, it will be observed that the pressure distribution is still fairly uniform across the span, so that the pressure is estimated quite well by simply taking the two-dimensional wedge values.

Figure 17 gives an example of conditions below the design Mach number where at the design incidence the shock wave is detached. For the incidence range covered by the measurements, It will be seen that there is little variation of pressure over the inboard region, and the pressure coefficient is only some 10% below the calculated two-dimensional value.

The effect of sideslip angle β on the lower surface pressures has also been studied. The results for wings *N* and *O* are shown in Fig. 18, both wings being at their design incidence and Mach number. With sideslip the shock wave is weakened at the advancing leading edge while it becomes stronger at the retreating edge and eventually becomes detached. Calculated pressures are seen to be in good agreement with the measured values for wing *N* which is conically supersonic for the conditions shown. It is apparent that the pressure distribution is sensitive to sideslip near the leading edges; nevertheless for the particular wing designs tested the surface pressures remain fairly uniform over the inboard regions.

Typical vapour screen pictures for wing *R* are shown in Fig. 19:

(*a*) shows the design condition with a very nearly plane shock wave,

(*b*) corresponds to 8° incidence, and again the shock wave has very little curvature, and

(*c*) shows the case of 4° of sideslip where the shock wave has considerable curvature.

In summary, the supersonic wind-tunnel tests showed that a uniform undersurface flow can be achieved with these simple geometric shapes, and that this uniform flow can be retained over a wide range of off-design incidence and Mach number. However, the uniformity of the flow is sensitive to small angles of sideslip.

4. Hypersonic Wind-Tunnel Tests of Simple Delta Wings

Pressure distributions over three delta wings of aspect ratio unity have been measured in the R.A.E. 7 in × 7 in hypersonic wind-tunnel at a Mach number of 8·6. The purpose here was to compare a caret wave-rider with some simple flat-bottomed delta wings which all have an aspect ratio of one

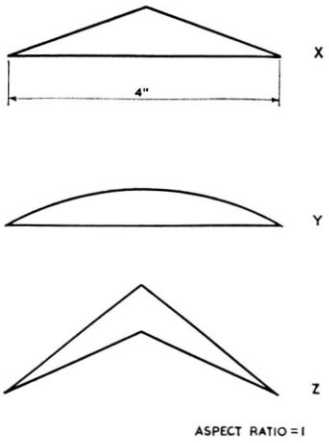

FIG. 20 — Delta models tested in hypersonic tunnel

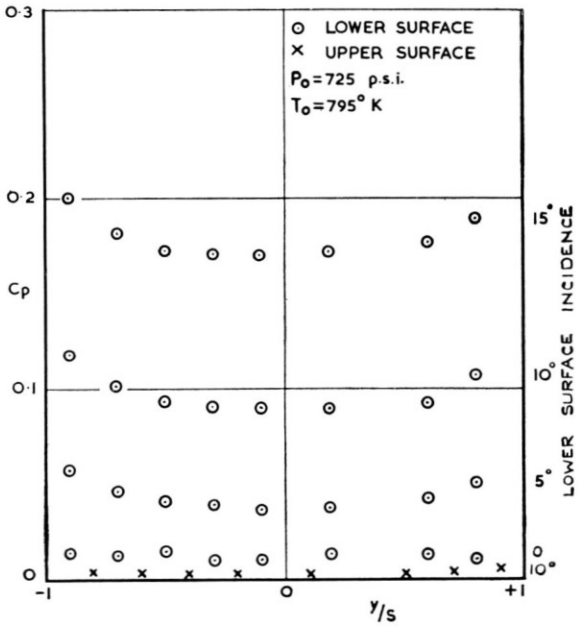

FIG. 21(*a*) — Spanwise pressure distribution on delta wing (model *X*)
$M_\infty = 8{\cdot}6$, $(\mathrm{Re})_c = 1{\cdot}58 \times 10^6$

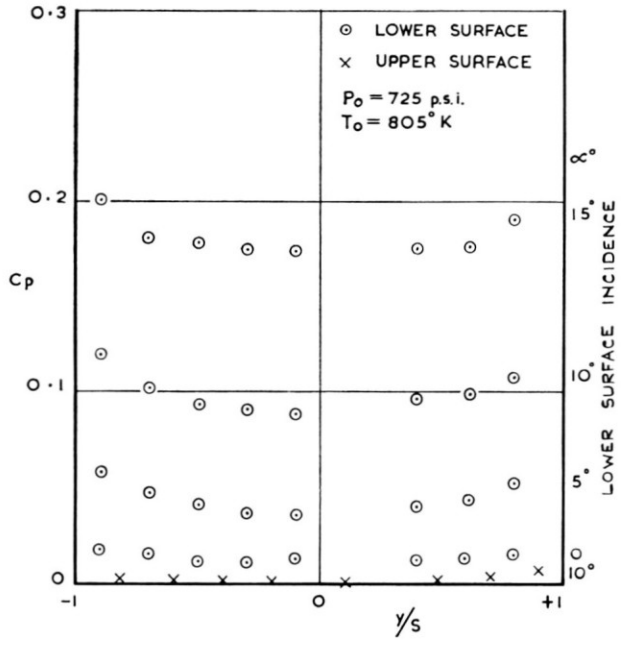

FIG. 21(*b*) — Spanwise pressure distribution on delta wing (model *Y*)
$M_\infty = 8{\cdot}6$, $(\mathrm{Re})_c = 1{\cdot}55 \times 10^6$

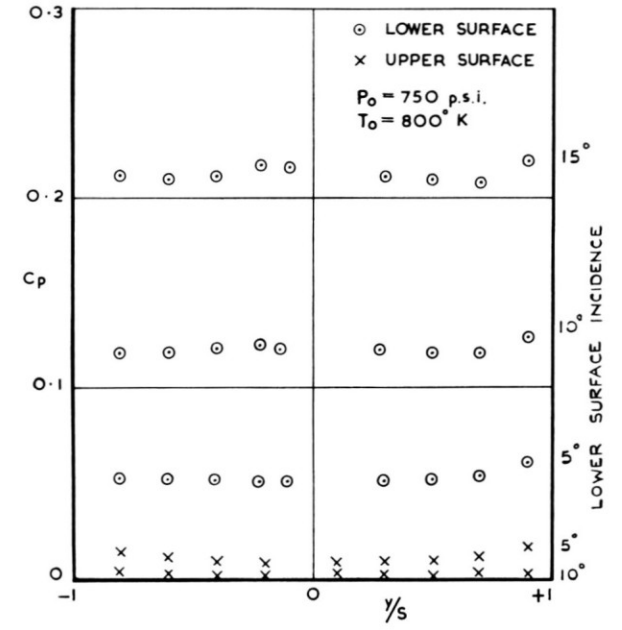

FIG. 21(*c*) — Spanwise pressure distribution on caret wing (model *Z*)
$M_\infty = 8{\cdot}6$, $(\mathrm{Re})_c = 1{\cdot}4 \times 10^6$

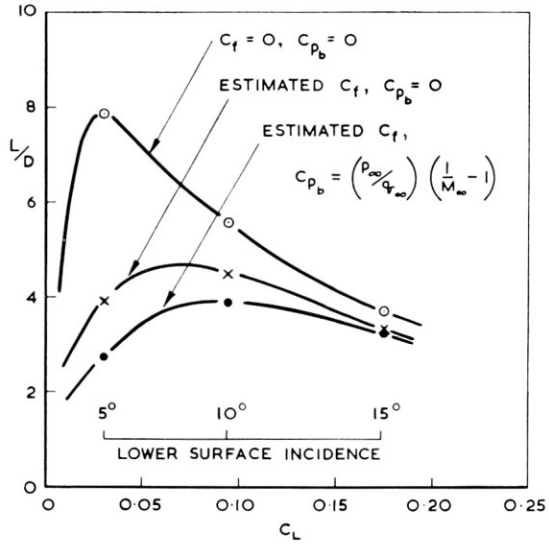

FIG. 22(*a*) — Lift to drag ratios for delta wing (model *X*)
$M_\infty = 8{\cdot}6$, $(\mathrm{Re})_c = 1{\cdot}58 \times 10^6$

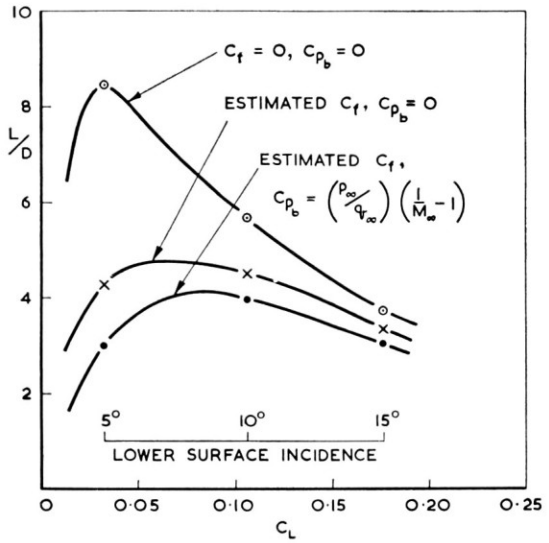

FIG. 22(*b*) — Lift to drag ratios for delta wing (model *Y*)
$M_\infty = 8{\cdot}6$, $(\mathrm{Re})_c = 1{\cdot}55 \times 10^6$

and a volume coefficient, τ of 0·06. Details of the three models† are given in Fig. 20, and the tests will be fully reported in ref. 6. Typical spanwise pressure distributions at $x/c = 0{\cdot}62$ are shown in Fig. 21. The caret wing is seen to have a reasonably uniform pressure over the lower surface for quite a wide range of angles of incidence, but the two flat-bottomed deltas show a steep rise in C_p towards the tips, particularly at the higher incidences.

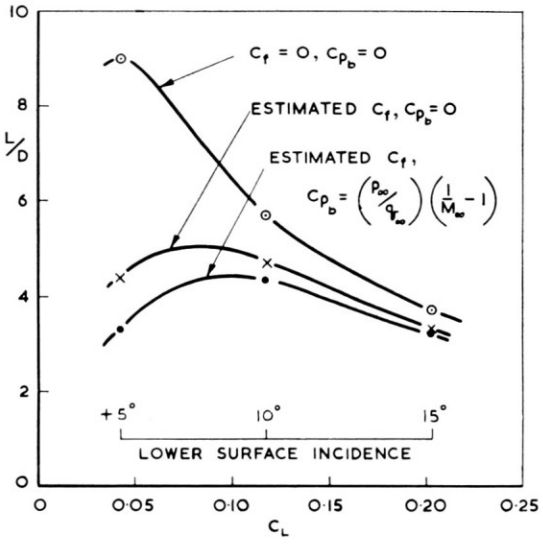

FIG. 22(*c*) — Lift to drag ratios for caret wing (model *Z*)
$M_\infty = 8{\cdot}6$, $(\mathrm{Re})_c = 1{\cdot}4 \times 10^6$

The pressure distributions have been integrated to give the L/D ratios shown in Fig. 22. Skin friction drag has been estimated by methods given in refs. 10 and 11, and a simple empirical relation (*see* ref. 1) has been used to show the effect of base pressure. For cruise conditions the appropriate curves are those for zero base pressure drag since the base will be effectively filled by the propulsive jet. Fig. 22 shows that the caret wing model has a slightly superior performance over the other two models and a maximum lift to drag ratio of about 5 is achieved. It is worth noting that this occurs at a relatively low value of C_L, but the maximum is fairly flat.

It now remains to show the range performance that may be achieved with L/D's of this order, and this is done in the next section.

† Further geometric details of model *Z* are given in Table I.

5. Range Performance of Hypersonic Aircraft

It is not possible to optimise the design of long-range hypersonic aircraft on cruise performance alone, since a considerable part of the total range may be covered during the climb and final glide phases of the flight plan. This has been taken into account in some recent calculations of the range performance of hypersonic aircraft[7] using hydrogen fuel. Two different estimates of specific fuel consumption were used in the calculations, one representing perhaps the ultimate performance that may be achieved, the other being a reasonable extrapolation of current values. Both estimates assume the use of a supersonic combustion ramjet for cruise Mach numbers above 6. Some of the results are given in Figs. 23 and 24. These show the ratio of fuel weight to

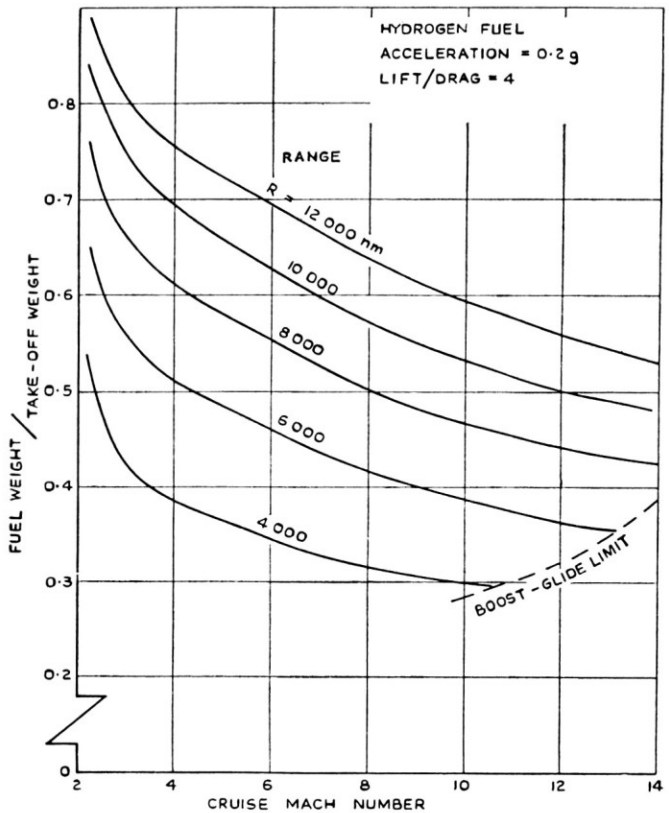

Fig. 23 — Variation of fuel fraction with range and cruise Mach number ($L/D = 4$)

take-off weight plotted against the cruise Mach number for various values of total range. Fig. 23 assumes a constant value of the lift to drag ratio of 4 and the less optimistic assumption for s.f.c., whereas Fig. 24 assumes an L/D of 6 and the optimistic estimate of s.f.c. Even in the former case it appears that

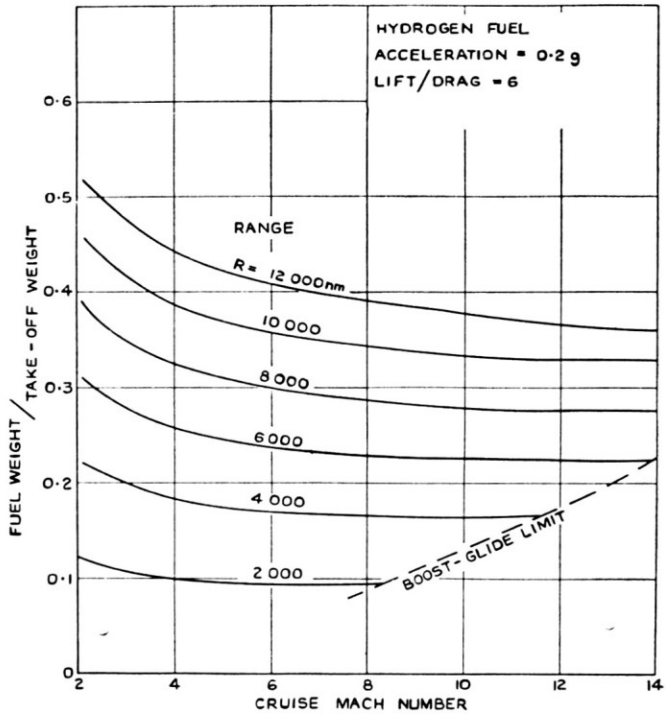

FIG. 24 — Variation of fuel fraction with range and cruise Mach number ($L/D = 6$)

ranges of the order of 10,000 nm may be possible for values of L/D above 4 and a fuel weight of no more than 50% of the take-off weight — this latter being a typical fraction for present-day subsonic jet transports.

Naturally, the use of hydrogen fuel entails a possible penalty because of the extra volume of fuel tankage required, which would lead to a reduction in lift to drag ratio. However, the calculations showed that the penalty need not be large for a large (say, 300,000–400,000 lb) aircraft, provided the wing loading is not too high. This conclusion is illustrated in Fig. 25.

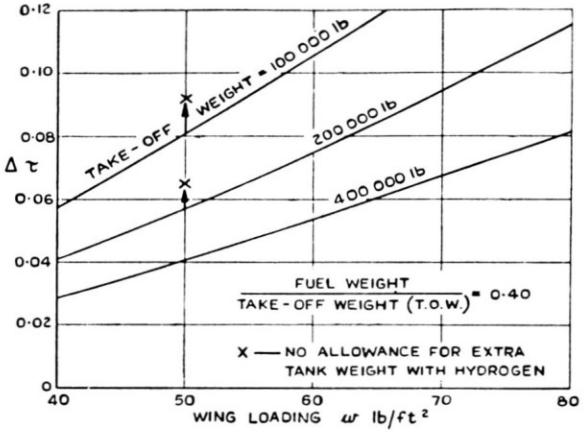

(*a*) Constant fuel weight/T.O. weight = 0·4

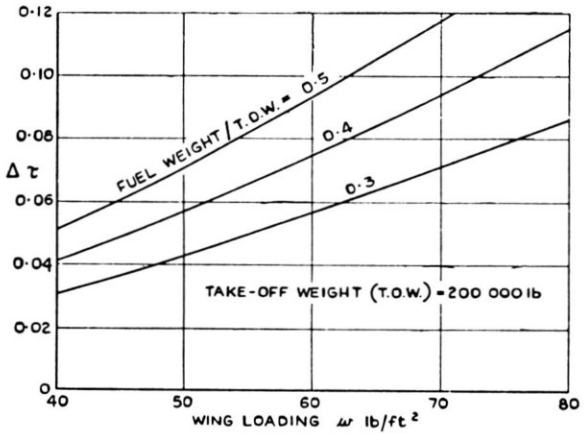

(*b*) Constant T.O. weight = 200,000 lb

FIG. 25 — Increase of volume coefficient with use of liquid hydrogen fuel instead of kerosine

6. CONCLUSIONS

Wind-tunnel tests over a wide Mach number range have been carried out on a series of geometrically simple shapes which may form the basis for the rational design of a practical hypersonic aircraft.

The low-speed tests indicated that these shapes introduce no particular difficulty in providing acceptable handling qualities in the landing condition.

The supersonic wind-tunnel tests showed that a uniform under-surface flow can be achieved with simple caret wave-rider shapes and that this uniform flow can be retained over a wide range of off-design incidence and Mach number.

Finally, the hypersonic tests showed that values of lift to drag ratio of over 4 can be readily achieved and calculations show that this enables ranges of the order of 10,000 nm to be obtained using liquid hydrogen fuel. This exciting prospect emphasises the need for continuing research in the materials, structures and propulsion fields to see if this aerodynamic performance potential can be realised in practice.

Acknowledgment

British Crown copyright, reproduced with the permission of the Controller, Her Brittanic Majesty's Stationery Office.

References

(1) Küchemann, D., 'Hypersonic aircraft and their aerodynamic problems.' *Progress in Aeronautical Sciences*, **6**, 271–354. Pergamon Press, 1965.
(2) Crabtree, L. F., 'Boundary layer effects on hypersonic aircraft.' *Jahrbuch der WGLR*, 1965.
(3) Keating, R. A., Mayne, B. L., 'Low speed characteristics of wave-rider wings. R.A.E. Technical Report *to be published.*
(4) Jones, J. G., 'A method for designing lifting configurations for high supersonic speeds using the flow fields of non-lifting cones.' R.A.E. Report No. Aero 2674, A.R.C. 24846, 1963.
(5) Treadgold, D. A., 'Off-design characteristics of caret wings.' Unpublished M.O.A. Report.
(6) Crane, J. F. W., 'Hypersonic tunnel tests of some geometrically simple lifting shapes.' Unpublished M.O.A. Report.
(7) Peckham, D. H., Crabtree, L. F., 'The range performance of hypersonic aircraft.' R.A.E. Technical Report No. 66178, 1966.
(8) Treadgold, D. A., 'Experimental study of the flow over a particular after-body shape having a near-sonic ridge line.' A.R.C. Current Paper 546. 1960.
(9) Picken, J., Greenwood, G. H., 'Free-flight measurements of heat transfer and observations of transition on a caret wing at Mach numbers up to 3·6.' R.A.E. Technical Report No. 65237, A.R.C. 27820. 1965.
(10) Crabtree, L. F., Dommett, R. L., Woodley, J. G., 'Estimation of heat transfer to flat plates, cones and blunt bodies.' R.A.E. Technical Report No. 65137. 1965.
(11) Collingbourne, J. R., Peckham, D. H., 'The lift and drag characteristics of caret wings at Mach numbers between 5 and 10.' R.A.E. Technical Report No. 66036. 1966.

Discussion

J. Manee (N.L.R., Amsterdam, The Netherlands): Dr. Crabtree has mentioned in his section about the low speed characteristics that the pitch-up following the early vortex breakdown as found for the delta wing *A* can be reduced by blunting the apex. However, as indicated in Fig. 5 this reduction has to be paid for by a rotation of the pitching moment curve in an unstable sense. Will this effect not make it very difficult to cope with the centre of gravity position with respect to longitudinal stability for a planform with a blunt apex?

L. F. Crabtree and D. A. Treadgold: One of our main outstanding problems is to obtain a practical volume distribution, as is mentioned in the Introduction. However, the shapes tested so far really represent only the front part of a practical aircraft. When the combustion section and exhaust nozzle are integrated with the intake section the problem may be very much easier.

P. G. Pugh (N.P.L., Teddington, U.K.): I note that all the configurations tested had sharp leading edges. These would, in practice, have to be blunted in order to ameliorate kinetic heating. What the effects would this have on maximum lift/drag ratio?

Second, what are the particular advantages of the lower surface flow uniformity which the authors have demonstrated can be obtained over a wide range of test conditions?

I am very interested to learn that the former question will be the subject of forthcoming tests at R.A.E.

L. F. Crabtree: In my paper on boundary layer effects on hypersonic aircraft published in *Jahrbuch* 1965 *der W.G.L.* I reported some work carried out by Capey which showed that only a small amount of leading-edge blunting was required, provided it was made from a solid slab of material of high thermal conductivity. However, our programme of future work included a study of the effects of leading-edge blunting since it is still an important problem.

The advantages of maintaining a constant under-surface pressure are given in detail in the paper. I might just emphasise here that one example is the possibility of maintaining large areas of laminar flow since with straight streamlines there would be no secondary instability of the boundary layer of the type discovered by Gray on conventional swept wings. In fact, the hypersonic caret-wing aircraft may provide the first successful and natural laminar flow aircraft.

R. C. Lock (N.P.L., Teddington, U.K.): I should like to ask if any comparisons have been made for caret wings, in off-design conditions such that the flow is conically elliptic, between the experiments described in this paper and the recent theoretical work on this subject by Dr. L. C. Squire at Cambridge University? He has developed an improved form of second-order Newtonian theory which has shown remarkably good agreement with experimental results on wings very similar to those tested by the authors, and at Mach numbers as low as 4.

D. A. Treadgold: No comparisons have yet been made with Dr. L. C. Squires' recent method, which I understand is to be published shortly in *The Aeronautical Quarterly* ('Calculated pressure distributions and shock shapes on thick conical wings at high supersonic speeds'). He has obtained numerical solutions of the integral equation given by Messiter and Hida (ref. *A.I.A.A. Journal*, Vol. 1, pp. 794–801 and Vol. 3, pp. 427–433) for a variety of conical shapes, including an example of a caret wing. His results look very encouraging and he has been approached to develop his method further, and to apply it to the examples covered by the tests described in the paper.